Locally self-consistent Green's function approach to the electronic structure problem

I. A. Abrikosov, S. I. Simak, and B. Johansson
Condensed Matter Theory Group, Department of Physics, Uppsala University, S-75121 Uppsala, Sweden

A. V. Ruban and H. L. Skriver
Center for Atomic-scale Materials Physics and Department of Physics, Technical University of Denmark, DK-2800 Lyngby, Denmark
(Received 14 March 1997)

The locally self-consistent Green's function (LSGF) method is an order-N method for calculation of the electronic structure of systems with an arbitrary distribution of atoms of different kinds on an underlying crystal lattice. For each atom Dyson's equation is used to solve the electronic multiple scattering problem in a local interaction zone (LIZ) embedded in an effective medium judiciously chosen to minimize the size of the LIZ. The excellent real-space convergence of the LSGF calculations and the reliability of its results are demonstrated for a broad spectrum of metallic alloys with different degree of order. The relation of the convergence of our method to fundamental properties of the system, that is, the effective cluster interactions, is discussed. [S0163-1829(97)06740-4]

I. INTRODUCTION

Within the past two decades, density functional theory[1] (DFT) has become a standard method of calculation in several branches of physics, including that of calculating ground-state properties of solids. In the latter branch almost all calculations rely on the Kohn-Sham approach[2] in which one solves a set of effective one-electron equations with a particular choice of basis functions. In a periodic system this leads to a Hamiltonian matrix, which upon Fourier transformation to reciprocal k space has a dimension proportional to the number of atoms N in the unit cell. The computational effort of the corresponding eigenvalue problem scales approximately as $O(N^3)$ and most current DFT methods are therefore limited to unit cells with a few hundred atoms. Hence, if one needs to calculate the total energy of several thousand atoms, as one may in studies of local environment effects in alloys or simulations of nanoscale materials, the scaling properties of the computational technique must be improved.

Several computational techniques with better scaling properties, so-called $O(N)$ methods for DFT, have been proposed.[3–22] They are all based on the assumption, tacitly assumed in most solid-state calculations, that a change in an external potential at sufficiently large distances has no effects on the property, e.g., the total energy, under consideration. One example is the neglect of surface effects in ordinary bulk calculations. This has been elevated recently to a principle of nearsightedness[22] and should not be confused with the length scale expressed, for instance, in the form of localized orbitals,[3–7] short-ranged density matrices,[8–12] or tight-binding models.[13–15]

The $O(N)$ techniques based on a Green's function approach in Refs. 14 and 18–21 owe their favorable scaling properties to the fact that the electron density, which is the fundamental quantity in DFT, is obtained solely from the site-diagonal blocks of the Green's function matrix. It follows that the conventional approach, i.e., diagonalization of a Hamiltonian or inversion of a Green's function matrix, involves large amounts of data that are needed only by the mathematical diagonalization, hence the $O(N^3)$ scaling, and not by DFT in the construction of the electron density and total energy. As we shall show, the site-diagonal block of the Green's function matrix for a particular atom in a large system may be obtained with sufficient accuracy by considering only the electronic multiple scattering processes in a finite region of space containing M atoms and called the local interaction zone (LIZ).[19,20] This multiple scattering problem scales as $O(M^3)$, but when it is applied, in turn, to each atom in the unit cell the combined computational procedure exhibits the desired linear scaling in N with a prefactor determined by M and by the number of basis functions.

In the $O(N)$ methods based on the Green's function approach suggested in Refs. 14 and 18–20 this prefactor is determined either by the convergence of the truncated series of the recursion method[14,18] or by the real-space convergence of the multiple scattering processes of the locally self-consistent multiple scattering method.[19,20] In both cases, however, the system beyond the truncated region is neglected and one needs relatively large M values to obtain an accurate total energy. Recently, Abrikosov *et al.*[21] showed that the size of the LIZ and hence the computational effort may be considerably reduced by embedding the truncated region in an effective medium. This embedding may be established by means of the Dyson equation connecting the desired Green's function to the Green's function of a reference system that may have much higher symmetry than the system under consideration. The problem is thereby reduced to that of finding an effective medium that at the shortest possible distance is viewed by the central atom of the LIZ as the system under consideration, i.e., the effective medium that makes the central atom in the LIZ nearsighted.

In the present paper we discuss the recent locally self-consistent Green's function (LSGF) technique proposed by Abrikosov *et al.*[21] We make a detailed analysis of the technique and demonstrate that it is numerically efficient, scales linearly with the number of atoms in the system under consideration, and provides an equally adequate description of

ordered, random, and segregated phases. The analysis is illustrated by results for the total energy and state densities derived from a broad spectrum of intermetallic compounds formed between simple, transition, and noble metals having different crystal structures, degree of order, or tendency towards ordering. Where possible we compare our results with those obtained by other first-principles methods to justify the reliability and generality of the present LSGF method.

The LSGF method turns out to be especially fruitful and effective for systems with arbitrarily distributed atoms of several components on an underlying crystal lattice. In the LSGF such systems are modeled by a supercell with periodic boundary conditions and due to the order-N scaling of the computational efforts with respect to the size of the supercell we may choose this cell sufficiently large to represent the physical properties of the problem at hand. The efficiency is achieved by a combination of the concept of a local interaction zone, which leads to the order-N scaling, a judiciously chosen effective medium, which reduces the size of the local interaction zone and thereby reduces the prefactor in the order-N scaling, and the application of the linear one-electron methods of Andersen,[23] which typically reduces the computational effort by an order of magnitude. The limitation is that one is restricted to a lattice supercell.

II. LOCALLY SELF-CONSISTENT GREEN'S FUNCTION METHOD

In this section we outline our $O(N)$ technique, which is based on a Green's function approach in conjunction with a linear muffin-tin orbital (LMTO) basis in the atomic sphere approximation (ASA) of Andersen and co-workers.[23–27] We first write down the expression for the total energy in the local density approximation (LDA) and its spatial decomposition into atomic spheres. We then reformulate the problem in the Green's function language, which only requires the solution of the multiple scattering problem in a finite region of space, the LIZ, and thereby leads to an $O(N)$ technique. We subsequently introduce the concept of an effective medium and show how this may be used to obtain a minimal local interaction zone and lead to a considerable increase in computational efficiency. Finally, we show how the real-space convergence of $O(N)$ techniques of the present kind may be understood in terms of interatomic potentials and how these may be used to establish the optimal size of the LIZ for a given system.

A. Total energy in the ASA

Let us consider the problem of calculating the total energy of a system of N atoms in a supercell subjected to periodic boundary conditions such as illustrated in Fig. 1. We assume that the atoms may be of different types and distributed with a specified degree of order. Within the LDA to DFT (Refs. 1 and 2) we may solve the Kohn-Sham equations

$$\left(-\nabla^2+\sum_R V_R(\mathbf{r})\right)\psi_i(\mathbf{r})=\varepsilon_i\psi_i(\mathbf{r}), \tag{1}$$

where $\mathbf{r}$ is a radius vector, ψ_i is the one-electron wave function, ε_i is the corresponding one-electron energy, V_R is an atom centered effective potential, and the sum runs over the all atomic sites R in the system. Given the electron density

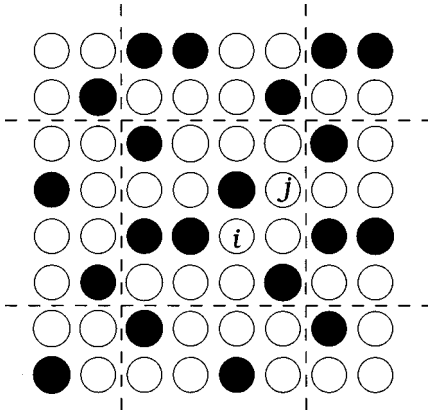

FIG. 1. In the LSGF method an infinite system with an arbitrary distribution of atoms of different kinds on an underlying crystal lattice is modeled by a supercell of N atoms with periodic boundary conditions.

$$n_R(\mathbf{r})=\sum_i^{occ}|\psi_i(\mathbf{r})|^2, \tag{2}$$

calculated from the solution to Eq. (1), the potentials V_R may be obtained in the ASA as[23,26]

$$V_R(\mathbf{r})=2\int_{S_R}d^3r'\frac{n_R(\mathbf{r}')}{|\mathbf{r}-\mathbf{r}'|}-\frac{2Z_R}{r}+V_{xc}[n_R(\mathbf{r})]+\frac{1}{S}\sum_{R'}M_{RR'}Q_{R'}. \tag{3}$$

Here the integral is over the atomic sphere of radius S_R centered at $\mathbf{R}$, Z_R is the atomic number of the atom at $\mathbf{R}$, n_R is the electron density obtained from the Kohn-Sham one-electron wave functions, V_{xc} is the exchange-correlation potential, S the average Wigner-Seitz radius, $M_{RR'}$ is the Madelung matrix for the supercell of N atoms, and Q_R is the net charge of an atomic sphere given by

$$Q_R=\int_{S_R}d^3r n_R(\mathbf{r})-Z_R. \tag{4}$$

With the above assumptions the desired total energy per atom may be calculated as the average over all N atoms in the system, i.e.,

$$E_{\mathrm{tot}}=(N)^{-1}\sum_{R=1}^{N}E_R, \tag{5}$$

where the site projected energy E_R has the form[26]

$$E_R=\int^{E_F}dEEN_R(E)-\int_{S_R}d^3r n_R(r)V_R(r)+\int_{S_R}d^3r n_R(r)\times\left(\int_{S_R}d^3r'\frac{n_R(\mathbf{r}')}{|\mathbf{r}-\mathbf{r}'|}-\frac{2Z_R}{r}+\epsilon_{xc}[n_R(r)]\right)+\frac{1}{2S}\sum_{R,R'}M_{RR'}Q_RQ_{R'}. \tag{6}$$

Here $N_R(E)$ is the local state density at site R calculated from the one-electron spectrum of Eq. (1), ϵ_{xc} the exchange-correlation energy density, and E_F the Fermi energy. A detailed derivation of the total energy expression in the ASA, LDA, and frozen core approximation has been given for the impurity case by Gunnarsson *et al.*[26]

B. Green's function formulation

The Kohn-Sham equations (1) and (2) may be formulated in terms of Green's functions. This problem has been discussed by a number of authors.[28–30] Within the LMTO formalism the two equations are replaced by[26]

$$[\mathbf{P}(z)-\mathbf{S}(\mathbf{k})]\mathbf{g}(\mathbf{k},z)=\mathbf{1}, \tag{7}$$

and

$$n_R(\mathbf{r})=\oint^{E_F}\frac{i}{\pi}G(\mathbf{r},\mathbf{r},z)dz. \tag{8}$$

Here $\mathbf{P}$ is the diagonal LMTO potential-function matrix, $\mathbf{S(k)}$ the structure constant matrix in the tight-binding representation, and $\mathbf{g}(\mathbf{k},z)$ the Korringa-Kohn-Rostoker (KKR) -ASA Green's function matrix in reciprocal space and defined for a complex energy z. The corresponding real-space Green's function $G(\mathbf{r},\mathbf{r},z)$ may be obtained from g as[26,29]

$$\begin{aligned}G(\mathbf{r}+\mathbf{R},\mathbf{r}'+\mathbf{R}',z)&=\sum_L\frac{\phi_l(r,C_l)\phi_l(r',C_l)}{z-C_l}Y_L(\hat{r})Y_L(\hat{r}')\delta_{RR'}\\&+\sum_{L,L'}\phi_l(r,z)\dot{P}_l(z)^{1/2}Y_L(\hat{r})[g_{RL,R'L'}(z)\\&-P_l(z)^{-1}\delta_{L,L'}]\dot{P}_{l'}(z)^{1/2}\phi_{l'}(r',z)Y_{L'}(\hat{r}'),\end{aligned} \tag{9}$$

where $\mathbf{r}$ is restricted to the atomic sphere centered at $\mathbf{R}$, ϕ is a partial wave evaluated at the complex energy z or at the center C_l of the l band, Y is the lattice harmonics, $\dot{P}$ is the energy derivative of the LMTO potential function, and L is the combined angular-momentum quantum numbers (l,m). The real-space KKR-ASA Green's function matrix $g_{RL,R'L'}(z)$ that enters Eq. (9) is obtained from $\mathbf{g}(\mathbf{k},z)$ by integration over the Brillouin zone

$$g_{RL,R'L'}(z)=(V_{BZ})^{-1}\int_{BZ}d\mathbf{k}e^{i\mathbf{k}\cdot(\mathbf{T}-\mathbf{T}')}g_{UL,U'L'}(\mathbf{k},z), \tag{10}$$

where $\mathbf{U}$ is a basis vector of the unit cell and connected to the lattice site $\mathbf{R}$ by a translation $\mathbf{T}$, i.e., $\mathbf{R}=\mathbf{U}+\mathbf{T}$.

The most efficient way to obtain the necessary electron density is provided by the LMTO one-center expansion

$$\begin{aligned}n_R(r)=(4\pi)^{-1}\sum_L\{&[\phi_{Rl}(r)]^2m^{00}_{RLL}\\&+2[\phi_{Rl}(r)\dot{\phi}_{Rl}(r)]m^{10}_{RLL}+[\dot{\phi}_{Rl}(r)\dot{\phi}_{Rl}(r)\\&+\phi_{Rl}(r)\ddot{\phi}_{Rl}(r)]m^{20}_{RLL}\},\end{aligned} \tag{11}$$

written in terms of the partial waves $\phi(r)$ of angular momentum l, their energy derivatives $\dot{\phi}(r)$ and $\ddot{\phi}(r)$, and the moments of the state density calculated as the contour integral over the occupied valence states

$$m^{q'q''}_{RL'L''}=\frac{1}{2\pi i}\oint^{E_F}dz(z-E_{\nu Rl'})^{q'}G^{\gamma}_{RL',RL''}(z)(z-E_{\nu Rl''})^{q''}, \tag{12}$$

where $E_{\nu Rl}$ is the energy used in the LMTO expansion. In this case the real-space Green's function matrix G^{γ} is obtained from $\mathbf{g}$ by the LMTO transformation theory[24] and the relevant equations for the present implementation may be found in Ref. 31. Finally, the sum of the one-electron energies may be obtained from

$$\int^{E_F}dEEN_R(E)=\sum_R\sum_L(E_{\nu Rl}m^{00}_{RLL}+m^{10}_{RLL}) \tag{13}$$

and we have the necessary information to calculate the total energy (6).

A direct solution of the Kohn-Sham equations in the conventional formulation (1) using a basis with N_L orbitals per atom requires the solution of an eigenvalue problem of order $N\times N_L$, the computational effort of which scales approximately as $O(N^3)$. Similarly, a direct solution of the Kohn-Sham equations in the Green's function formulation (7) requires the inversion of matrices $[\mathbf{P}-\mathbf{S}]$ also of order $N\times N_L$ and the computational effort again scales approximately as $O(N^3)$. Hence, so far we have gained nothing in terms of computational efficiency relative to the conventional formulation.

At this stage we note that it is only the site-diagonal block G^{γ}_{RR} (or g_{RR}) of the Green's function matrix that is required in the construction of the key quantities, i.e., electron density and total energy, through the energy moments of the state density (12). It follows that if there exists a procedure whereby only G^{γ}_{RR} may be calculated without the inversion of the complete Green's function implied in Eq. (7), one has sufficient information for the LDA self-consistency procedure.

C. $O(N)$, local interaction zone, and effective medium

The experience gained in the application of real-space cluster methods in electronic structure calculations shows that for a large cluster the properties of an atom deep inside the cluster are very close to those given by band structure methods. This suggests that the electron density and the density of states on a particular atom within a large condensed system may be obtained with sufficient accuracy by considering only the electronic multiple scattering processes in a finite spatial region centered at that atom. As a result, one may introduce the concept of a local interaction zone applied by Nicholson *et al.*[19,20] in the framework of the locally self-consistent multiple scattering (LSMS) method and later by Abrikosov *et al.*[21] in their preliminary account of the present work. The latter authors also introduced the concept of an effective medium, which we shall now describe.

Let us choose a reference system, which we will call the effective medium, by placing effective atoms on the lattice underlying the original supercell shown in Fig. 1. The effec-

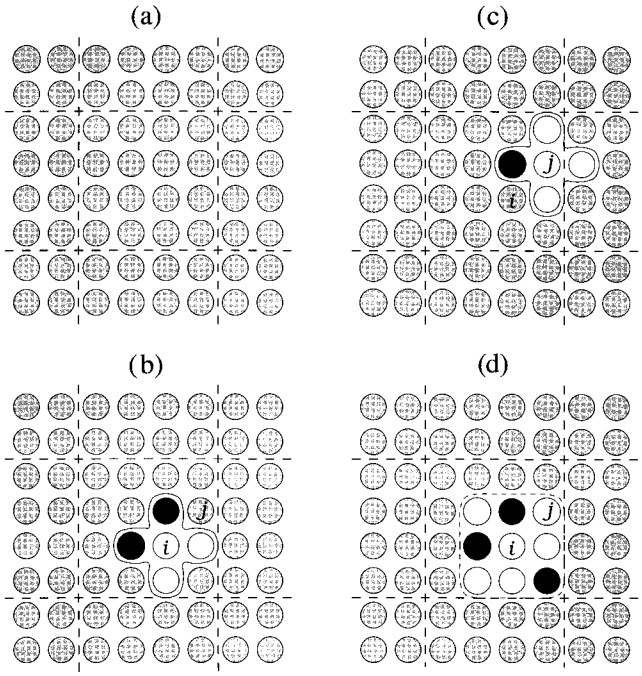

FIG. 2. Main idea of the LSGF method. In (a) we show effective atoms distributed on the same underlying lattice as the atoms of the original system in Fig. 1. The local interaction zone around site i, embedded in the effective medium, is shown in (b). In (c) the LIZ is moved to another site j and it will be moved through all the sites of the supercell. Note that the distribution of atoms in the LIZ is essentially the same as in the original system and we make use of the periodic boundary conditions when forming the LIZ for the atoms close to the boundaries of the supercell. The size of the LIZ can be different, as shown in (d), and it depends on the types of the atoms constituting the alloy, on the degree of order, etc., but not on the size of the supercell. See the text for a complete discussion.

tive atoms are represented by their potential functions $\widetilde{P}_R$, which on the average describe the properties of the original system as close as possible, and their Green's function $\widetilde{g}$ may be obtained from $\widetilde{P}_R$ and the structure constants $\widetilde{\mathbf{S}}$ of the underlying lattice by solving Eq. (7) in the conventional manner. Since the effective medium constructed in this way has the full symmetry of the underlying lattice and may be specified by a small unit cell containing $\widetilde{N}$ effective atoms, the corresponding matrix inversion problem is only of order $\widetilde{N}\times N_L$. Hence the computational effort of constructing the effective medium, which scales as $O(\widetilde{N}^3)$, may be neglected in the limit $N\gg\widetilde{N}$.

Following Nicholson *et al.*,[19,20] we now surround an atom at site R by $M-1$ neighboring atoms, forming an M-atom local interaction zone. However, instead of solving the local multiple scattering problem directly, as it is done in the LSMS method, we embed each local interaction zone in the effective medium constructed above. The procedure is illustrated in Fig. 2. As a result, the Green's function for the LIZ is now given by the Dyson equation, which for the Green's function matrix g_{RR} at the central site R may be written as

$$g_{RR}=\widetilde{g}_{RR}+\sum_{R'=1}^{M}\widetilde{g}_{RR'}(\widetilde{P}_{R'}-P_{R'})g_{R'R}, \qquad (14)$$

where the sum runs over the M atoms in the LIZ.[32] Note that, although the entire Green's function matrix $g_{R'R}$ does not in general correspond to that of the system under consideration, the site-diagonal block g_{RR} will approach that of the real atom at R for a sufficiently large LIZ. In this sense g_{RR} will be locally self-consistent. The matrix problem in Eq. (14) is of order $M\times N_L$ and the computational effort scales as $O(M^3)$, which upon a judicious choice of the effective medium may be considerably reduced relative to the conventional $O(N^3)$ procedure (7).

Since it is only the site-diagonal blocks of the Green's function matrix that are needed to determine the charge density, the one-electron potential, and the total energy of the supercell, we may now devise the following $O(N)$ method. Calculate g_{RR} for a particular atom in the supercell by forming the associated LIZ and solving Eq. (14). Then move to a different atom and repeat the procedure. Continue until the atoms in the supercell have been exhausted. Thereby, the solution of the Kohn-Sham equations (7) for the entire N-atom system is decomposed into N independent problems. The procedure is clearly one way to calculate the site-diagonal blocks of the Green's function matrix for the entire N-atom system without calculating a large number of unimportant off-diagonal elements and without introducing approximations such as the diagonal disorder model.

The computational effort of the complete procedure scales as $O(NM^3)$ and we expect the size of the elementary computational problem connected with the LIZ, i.e., M, to depend on the atomic species, the underlying lattice, but not on N. We note that the N elementary problems are independent of each other and that the algorithm therefore is ideal for implementation on massive parallel computers.

D. Choice of effective medium

Provided one applies a sufficiently large LIZ, the local interaction-zone concept does not include any new approximations in the solution of the KKR-ASA equations (7) and the introduction of an effective medium may be seen as a device to reduce the size of the LIZ as much as possible. Since the Dyson equation is exact, there exists a number of different choices for the effective medium, all of which will lead to the same solution to Eq. (7) but have different convergence properties in real space. One may therefore try to find an effective medium that is localized in the sense that $\widetilde{g}_{RR'}\ll 1$ for R' outside the smallest possible LIZ centered at R; and in that case the summation in Eq. (14) may be truncated at a very small M value. However, there exists a minimum length D that is the range over which a perturbation, such as a single impurity in an ideal host[28,26,29,33] or an interface,[34–38] makes its presence felt, and this ultimately determines the size of the LIZ that may therefore be larger than the range over which $\widetilde{g}_{RR'}$ is localized. We discuss this issue in Sec. II E.

In choosing an effective medium we try to satisfy three criteria. First, we look for an effective medium with scattering properties as viewed by from the central atom of the LIZ as close as possible to those of the supercell system at the shortest possible distance. Second, the Green's function of the effective medium must be localized in real space at the range of the screening length D of a perturbation in the po-

tential energy. Finally, we require the effective medium to be as simple as possible, i.e., a single site.

If we consider the trivial example of a monatomic solid with a Bravais lattice, e.g., fcc Cu, one may immediately specify a perfect effective medium. We simply identify the effective atoms with the host Cu atoms, and in this case a LIZ with $M=1$, i.e., a single-site LIZ including only the atom at R, is sufficient for an exact solution of the electronic structure problem. If, on the other hand, we consider an ordered or partially ordered intermetallic compound, e.g., NiAl in the $B2$ structure, there are at least two obvious choices for the effective medium. First, one may view the compound as a distribution of atoms on the underlying $B2$ lattice with two types of effective atoms, one for the α (i.e., Ni) sublattice and another for the β (i.e., Al) sublattice. This will, by definition, lead to a single-site LIZ, essentially as in the previous case of a pure element. However, the effective medium itself becomes more complicated because the unit cell of the underlying lattice consists of two atoms. Alternatively, one may view the compound as a distribution of atoms on an underlying bcc lattice with one type of effective atom that must be defined as some kind of ''average'' atom.

The last example leads us to the well-known alloy problem with its hierarchy of single-site approximations for the effective medium increasing in accuracy from the virtual crystal approximation over the average t-matrix approximation (ATA) to the coherent potential approximation (CPA).[39] All of these approximations may be used to generate the effective medium, and we will specifically compare the numerical results obtained with the ATA and CPA effective media in Sec. VI B. From the experience gained in the study of alloys one expects the CPA to lead to the fastest convergence with respect to the size of the LIZ, at least for completely random alloys. In fact, the CPA effective medium fulfills all three criteria listed above and in particular gives a very good description of the scattering properties of a completely random alloy, whereby the central atom of the LIZ starts to ''see'' the effective medium as the real system as soon as an interchange of alloy components on the lattice sites becomes unimportant. This should be contrasted with the conventional $O(N)$ schemes where the central atom does not see anything beyond its own LIZ. Finally, the CPA Green's function decays, apart from an oscillating factor, exponentially as $R^{-1}e^{-R/l}$, where l is the mean free path,[40] and the CPA effective medium is a single site.

Our original goal is to calculate the total energy of N atoms in a supercell. Although this supercell may contain atoms of, for instance, only two types, say A and B, all the N atoms will in general be inequivalent due to differences in their local environment. These differences are completely ignored in the two component CPA, but may to some extent, restricted by the single-site approximation, be accounted for in the framework of the multicomponent generalization. For example, Johnson and Pinski employed this idea in their charge-correlated CPA.[41] Here we will define the effective medium to be used in the embedding of the LIZ as that given by the CPA for a multicomponent and, if necessary, multisublattice alloy. The number of components at each sublattice will be equal to the number of equivalent positions in the supercell formed from the underlying lattice, i.e., in the simplest case of a monatomic underlying lattice each atom in the supercell is considered to be a component of an N-atom alloy. On the other hand, in the $B2$ alloy mentioned above there will be $N_\alpha=\frac{1}{2}N$ components in the alloy formed by the sites of the α sublattice and $N_\beta=\frac{1}{2}N$ components in the alloy formed by the β sites. We thereby assume that the atoms are randomly distributed on their sublattices and neglect the fact that they occupy definite positions in the system. The difference between different atoms (or alloy components) will enter through their one-electron potentials.

To determine the potential functions for the effective atoms and the Green's function of the effective medium one must solve the following system of coupled single-site equations for the α sites in the unit cell of the underlying lattice:[31,42]

$$\widetilde{g}_{\alpha\alpha}=(V_{BZ})^{-1}\int_{BZ}d\mathbf{k}\{[\widetilde{\mathbf{P}}-\mathbf{S}(\mathbf{k})]^{-1}\}_{\alpha\alpha},$$

$$g^0_{R\alpha}=\widetilde{g}_{\alpha\alpha}+\widetilde{g}_{\alpha\alpha}(\widetilde{P}_\alpha-P_R)g^0_{R\alpha},$$

$$\widetilde{g}_{\alpha\alpha}=(N_\alpha)^{-1}\sum_{R\in\alpha}g^0_{R\alpha}, \tag{15}$$

and similarly for the β sites. Here V_{BZ} is the volume of the Brillouin zone of the underlying unit cell and the integration is over the corresponding Brillouin zone. An efficient technique to solve these equations is discussed in the Appendix.

It is important to note that the Green's function $g^0_{R\alpha}$ defined in Eq. (15) is not equal to the desired Green's function g_{RR} because the former is determined by the solution of the single-site Dyson equation while the latter is the site-diagonal block of the Green's function matrix determined by the cluster, non-single-site Dyson equation (14) for the LIZ. Consequently, the LSGF method with the CPA effective medium must not be considered as a simple generalization of the CPA, such as the molecular CPA. In the present context the effective medium is used only to improve the convergence in real space, i.e., reduce the size of the local interaction zone. Hence it is unimportant whether or not the effective medium describes the average alloy properties exactly because a slightly larger LIZ may compensate for the inaccuracy. In addition, by keeping our effective medium a single site we obviously also keep the correct analytical properties of all the Green's functions involved in the LSGF technique, i.e., the effective medium Green's function and those for the LIZ.

E. Relation to interatomic interactions

The properties of the effective medium are not the only factors that determine the real-space convergence of a total energy calculation. In fact, it has been shown by Gunnarsson *et al.*[26] for the impurity case that to obtain an accurate change in the total energy upon the introduction of an impurity at a particular site one must sum only over the sites where the potential is perturbed. Although this range is smaller than the range of the perturbation of the wave functions, it may be larger than the localization range of the effective medium and thereby effectively determine the size of the LIZ. Here we demonstrate that the convergence of the total energy in the LSGF method is also governed by the

potential and that the size of the LIZ may be estimated from the range of the effective interatomic interactions. To do so we will apply a simplified model that, however, reflects the basic features of the physics outside of the effective medium and the LIZ concept.

Let us first consider a pure element in an ideal crystal lattice and assume that the total energy of a crystal with N sites may be written

$$E_{\rm tot}=\sum_{i=1}^{N}\epsilon_i, \tag{16}$$

where ϵ_i is the energy of the atom at the ith site, which in turn may be defined in terms of the interatomic potentials as

$$\epsilon_i=v_i^{(1)}+\frac{1}{2}\sum_{j\neq i}v_{ij}^{(2)}+\frac{1}{3!}\sum_{j\neq i;k\neq i,j}v_{ijk}^{(3)}+\cdots. \tag{17}$$

Here $v_i^{(1)}$, $v_{ij}^{(2)}$, and $v_{ijk}^{(3)}$ are the on-site interaction, pair potential, and three-body potential acting among atoms at sites i, j, and k and all summations run over the entire crystal. Without loss of generality we may assume that all many-body potentials starting from three-body terms vanish. At least they normally fall off much faster with distance than the pair potentials.

Similar to the LSGF method, we introduce a LIZ around each atomic site and inside this LIZ we have the real atoms of the system and outside we place effective atoms. If the LIZ includes n coordination shells, the energy of the central atom in each LIZ is given by

$$\epsilon_i^{(n)}=v_i^{(1)}+\frac{1}{2}\sum_{\xi=1}^{n}m_\xi v_\xi+\frac{1}{2}\sum_{\xi=n+1}^{\infty}m_\xi\tilde{v}_\xi, \tag{18}$$

where $v_\xi\equiv v_{ij}^{(2)}$ with j in the ξth coordination shell, $\tilde{v}_\xi$ is the pair potential between the real atom at i and an effective atom in the ξth coordination shell, and m_ξ is the coordination number. Therefore, an increase in the size of the LIZ by one coordination shell, i.e., from n to $n+1$, will cause the energy of each atom in the crystal to change by

$$\delta_i^{(n+1)}=\epsilon_i^{(n+1)}-\epsilon_i^{(n)}=\frac{m_{n+1}}{2}(v_{n+1}-\tilde{v}_{n+1}). \tag{19}$$

This is illustrated in Figs. 2(b) and 2(d), where the LIZ of two different sizes centered at the same site of the supercell are shown. Note that the regions inside the first shell of nearest neighbors and outside the second shell are the same in the two figures. Thus the only difference is found in the second shell, where the effective atoms in Fig. 2(b) are replaced by real atoms in Fig. 2(d).

Equation (19) shows that the convergence of the total energy with respect to the size of the LIZ is completely determined by the difference between the effective medium and the real system: The closer the effective medium is to the real system, the better the convergence. This means in particular that if one chooses a reference system with localized interatomic interactions for which $\tilde{v}_\xi=0$ starting from any coordination shell, one would in fact not achieve fast real space convergence because in this case the convergence is governed by the bare interatomic potentials $v(r)$. For simple metals these potentials are estimated in pseudopotential theory and they usually decay very slowly, $\approx\cos(2k_Fr)/r^3$ with distance r.[43,44] For transition metals the decay of the pair potentials may be estimated from surface calculations,[38] which show that the perturbation from the surface is completely screened at distances corresponding to seven to nine coordination shells. This agrees with the results of the LSMS method of Wang *et al.*,[20] in which the reference system is a free electron gas and hence $\tilde{v}_\xi=0$ for all shells.

In the case of a monotomic solid the convergence of the present LSGF method is trivial: The effective medium is the real atom, i.e., $\tilde{v}_{n+1}\equiv v_{n+1}$, and therefore $\epsilon_i^{(n)}\equiv\epsilon_i$, where ϵ_i is the exact value (17) of the energy of the atom on site i. To show the convergence of the LSGF method in the case of an alloy we consider a model alloy A_cB_{1-c} with two components under the condition that all the A atoms and all the B atoms in the crystal are equivalent. This is, for instance, the case for a completely ordered alloy with two type of sublattices, where the local environment of all the A sites as well as all the B sites is exactly the same. The effective medium in the LSGF method is now the completely random alloy of A and B atoms and therefore the change in the energy of an A atom upon an increase in the size of the LIZ by one coordination shell is

$$\begin{aligned}\delta_{iA}^{(n+1)}&=\epsilon_{iA}^{(n+1)}-\epsilon_{iA}^{(n)}\\&=\frac{m_{n+1}}{2}[c_{n+1}^{A}v_{n+1}^{AA}+(1-c_{n+1}^{A})v_{n+1}^{AB}-\tilde{v}_{n+1}^{AX}].\end{aligned} \tag{20}$$

Here v_{n+1}^{AB} is the pair potential between A and B atoms at the distance of the $(n+1)$th coordination shell, c_{n+1}^{A} the concentration of the A components in the $(n+1)$th coordination shell of the A atom, and $\tilde{v}_{n+1}^{AX}$ the pair potential between atom A and the chosen effective medium. If the effective medium is exactly that of the completely random alloy then $\tilde{v}_{n+1}^{AX}=cv_{n+1}^{AA}+(1-c)v_{n+1}^{AB}$, and if we note that for a given atomic distribution the concentration c_{n+1}^{A} may be expressed through the Warren-Cowley short-range order parameter α_ξ as $c_\xi^A=c+(1-c)\alpha_\xi$ we find that

$$\delta_{iA}^{(n+1)}=\frac{m_{n+1}}{2}(1-c)\alpha_{n+1}(v_{n+1}^{AA}-v_{n+1}^{AB}). \tag{21}$$

Similarly, we find the change in the total energy of atom B in the LIZ to be

$$\delta_{iB}^{(n+1)}=\frac{m_{n+1}}{2}c\alpha_{n+1}(v_{n+1}^{BB}-v_{n+1}^{AB}) \tag{22}$$

and therefore the change in the total energy of the whole crystal is

$$\begin{aligned}\delta E_{\rm tot}^{n+1}&=N[c\delta_{iA}^{(n+1)}+(1-c)\delta_{iB}^{(n+1)}]\\&=N\frac{m_{n+1}}{2}c(1-c)\alpha_{n+1}(v_{n+1}^{AA}+v_{n+1}^{BB}-2v_{n+1}^{AB}).\end{aligned} \tag{23}$$

We note that the last parentheses contain simply the effective pair interactions as defined in alloy theory and therefore the convergence of the total energy in the LSGF method in the

case of an alloy is exactly the same as the convergence of the effective interactions. However, it also depends on the degree of the order in an alloy.

In the case of a completely random alloy all the short-range-order parameters are zero, $\alpha_\xi = 0$, and it follows from Eq. (23) that it is sufficient to use a LIZ of only one atom, i.e., the single-site approximation, to find the exact value of the total energy. However, this is true only in the case where the chosen effective medium represents the random alloy of given species exactly, because Eq. (23) is derived under this assumption. In general, the condition $\tilde{v}^{AX}_{n+1} = c v^{AA}_{n+1} + (1-c) v^{AB}_{n+1}$ is not satisfied and one may only conclude that the difference in the total energy of the completely random alloy calculated by the LSGF method in the single-site approximation or ''exactly'' with a sufficiently large LIZ is given by the error in the approximation used in the definition of the effective medium of the completely random alloy. The numerical examples to be presented later show that the CPA in fact gives a good description of the electronic structure of a completely random alloy.

On the other hand, it is obvious from Eq. (23) that the worst possible convergence of the LSGF method should occur in a completely ordered alloy where all $\alpha_\xi \neq 0$. In this case the convergence of the total energy with respect to the LIZ size is reached at the distance over which the effective interactions in the system converge and the change of the total energy of a completely ordered alloy as a function of the LIZ size may be used as an estimate of the value of the corresponding effective pair interactions. However, since the Madelung potential and energy of the supercell in the LSGF method are determined exactly and independently of the LIZ size, such an estimate does not include the electrostatic contribution to pair interactions similar to those defined in Ref. 45. Finally, we note that the electrostatic contributions are also neglected in the generalized perturbation method (GPM).[40,46]

Concluding this section, we would like to point out that the LSGF method gives us the opportunity not only to check the convergence of the effective cluster interactions but also to calculate them and in particular to calculate *concentration-dependent* effective cluster interactions. This may be done by using the idea behind the well-known Connolly-Williams method.[47] That is, we calculate the total energies of alloys with different sets of correlation functions but for some fixed concentrations of the alloy components and then map these energies onto the corresponding cluster expansion. Since these calculations are fast one may perform a large number of them and thereby increase the accuracy of the interaction parameters obtained. The resulting effective cluster interactions will include not only the so-called band-energy term as in the GPM but all contributions to the total energy. Preliminary calculations have been carried out, but a discussion is beyond the scope of the present paper and will be presented elsewhere.

III. COMPUTATIONAL DETAILS

The complete self-consistent procedure of the LSGF-CPA method may now be summarized. We start with a guess for the charge density of all the atoms in the system. This could be a renormalized atomic density, but we find it more efficient to start from the result of a conventional CPA calculation for a random alloy with the same composition as the supercell. We then determine the potential function for the effective scatterers $\tilde{P}$ by solving Eq. (15) and constructing the effective medium Green's function for the LIZ by Eq. (10). Note that **U** in Eq. (10) is a basis vector in the unit cell of the underlying lattice. We proceed by solving Eq. (14) for each R. Now the site-diagonal blocks g_{RR} are known for all atoms in the system and we calculate the site-decomposed Green's function $G^{\gamma}_{RL',RL}(z)$, the moments of the state density Eq. (12), and the new charge density Eq. (11). Subsequently, we solve Poissons equation for the electrostatic potential, add the exchange-correlation potential, and repeat the procedure until self-consistency is reached.

The actual calculations were performed by means of the scalar relativistic LMTO method in the tight-binding representation employing s, p, and d orbitals in conjunction with the atomic sphere approximation.[23–27] The complex integrals were evaluated on a semi-circular contour using 16–25 energy points distributed so as to increase the sampling near the Fermi level. Exchange and correlation were included within the local density approximation using the Perdew-Zunger parametrization[48] of the many-body calculations of Ceperley and Alder.[49] The reciprocal space integrals were calculated by means of 200–500 k points in the irreducible part of the bcc or fcc Brillouin zone and the off-diagonal elements of the effective medium Green's function were constructed by means of the symmetrization technique described in Ref. 50. An effective two-step procedure for the charge self-consistency that speeds up the solution of the electronic structure problem by an order of magnitude is described in the Appendix.

IV. SUPERCELL APPROACH TO THE ALLOY PROBLEM

The efficiency of the LSGF method allows us to treat supercells with several hundred atoms of different types. Thereby the method is particularly suitable for the investigation of substitutional alloys over a broad spectrum of atomic configurations ranging from random to order with arbitrary degree of short-range-order effects. The question is now how one performs the necessary average over all possible configurations to determine the alloy properties of interest. Here we are helped by the principle of spatial ergodicity, according to which all possible finite atomic arrangements are realized in a single infinite sample. What makes this principle work in practice, in fact as well as the LSGF method itself, is the fact that for a given physical property $\mathcal{P}$, here the site-diagonal block of the one-electron Green's function matrix for each atom in the supercell, all the correlations in the atomic distribution become unimportant at some distance and hence the sample may be chosen finite.

The principle may be formulated more explicitly in terms of correlation functions Π_f, which are the Gibbs averages of the products of site occupation numbers in a particular geometrical configuration of sites, or a figure f. In the case of binary alloys it is convenient to determine the correlation functions as the product of spin variables s_i taking on values $+1$ and -1 depending on whether site i is occupied by one or the other component, i.e.,

$$\Pi_f = \langle s_i s_j \cdots s_k \rangle_f . \tag{24}$$

It was shown by Sanchez *et al.*[51] that any measurable property $\mathcal{P}$ of the system may be rigorously expanded in terms of the ensemble averages of the correlation functions (24)

$$\mathcal{P} = \sum_f \Pi_f p_f , \tag{25}$$

where summation runs over all possible figures. The coefficients p_f in the expansion (25), which are, for instance, the effective cluster interactions if $\mathcal{P}$ is the total energy, are usually nonzero only for some finite set of figures of nearest sites. This means that $\mathcal{P}$ is only sensitive to the atomic distributions inside the figures f for which $p_f \neq 0$, and to determine the quantity $\mathcal{P}$ corresponding to the ensemble average values of Π_f one may simply design a *finite* N-atom periodic structure, the distinct correlation functions $\tilde{\Pi}_f$ of which are equal to the ensemble average Π_f for all the figures for which $p_f \neq 0$. For all other figures the condition $\tilde{\Pi}_f = \Pi_f$ may be not satisfied, but this cannot influence the physical property $\mathcal{P}$.

The approach described above is the so-called special quasirandom structure (SQS) method suggested by Zunger *et al.*[52] and applied in the framework of conventional band structure techniques. Because of the problem with $O(N^3)$ scaling, only a few SQS's with $N \leqslant 32$ have been considered for fcc and bcc lattices for two concentrations, 50% and 25%, and for a completely random atomic distribution inside the first few coordination shells. The LSGF method allows us to calculate systems with up to 500 atoms even on a moderate workstation. With such a number of atoms in the supercell one may consider practically any random alloy composition with fixed correlation functions up to the sixth shell. Of course, the value of the concentration may only be rational fractions with an accuracy of $1/N$, but for many alloy problems such an accuracy is quite reasonable.

To generate a supercell with required correlation functions, we make use of a Metropolis-like algorithm. The N_k correlation functions that we want to match determine a vector $\boldsymbol{\xi}$ in an N_k-dimensional space. Starting from an arbitrary initial configuration corresponding to some vector $\boldsymbol{\xi}'$, a particular pair of atoms of different kind, chosen at random, is considered and a vector $\boldsymbol{\xi}''$ corresponding to an exchange of the two atoms is calculated. If the distance in the N_k-dimensional space between $\boldsymbol{\xi}''$ and $\boldsymbol{\xi}$ is less than the distance between $\boldsymbol{\xi}'$ and $\boldsymbol{\xi}$, the exchange is accepted; otherwise the initial configuration is kept. The procedure is repeated until we have generated a configuration sufficiently close to the one required. We point out that the manner in which the substitutional alloys are constructed is independent of the LSGF method itself. The former is a statistical problem, while the latter is a method to solve the electronic structure problem for a given supercell with a given atomic distribution.

V. NUMERICAL ASPECTS

A. Convergence with respect to the size of the supercell

Within the special quasirandom structure approach the question is how large the supercell has to be for the LSGF method to yield converged total energies. Here we show that in the case of a supercell with specified correlations the parameters that determine the convergence with respect to the size of the supercell are the correlation functions up to the range of nonzero effective cluster interactions. To do so, we choose two fcc alloys, $Cu_{50}Zn_{50}$ and $Cu_{75}Au_{25}$, where the most important effective interactions are those of the first coordination shell as discussed in Sec. II E. This means, as discussed in Sec. IV, that to model a completely random alloy in these systems it is sufficient to consider a small supercell and that an increase in system size will leave the total energy unchanged.

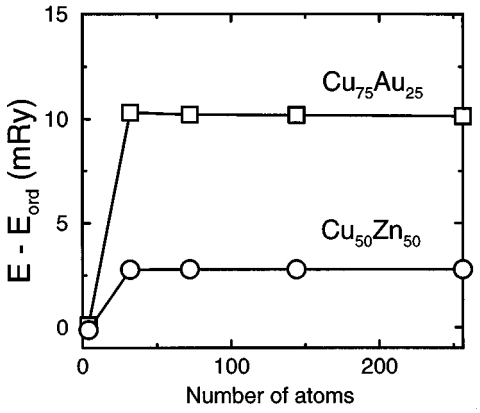

FIG. 3. Total energies of random fcc $Cu_{50}Zn_{50}$ (circles) and $Cu_{75}Au_{25}$ (squares) alloys calculated by the LSGF-CPA method relative to the energy of the corresponding ordered phase ($L1_0$ for Cu-Zn and $L1_2$ for Cu-Au) as a function of the number of atoms in the system. The energies for the ordered phases were calculated by the conventional LMTO-GF method. The Wigner-Seitz radii $R_{WS} = 2.70$ a.u. (Cu-Zn) and 2.80 a.u. (Cu-Au) were used for both the ordered and random alloys. The LIZ consists of one and two shells of nearest neighbors for the Cu-Zn and Cu-Au systems, respectively.

In Fig. 3 we present the calculated total energy of random fcc $Cu_{50}Zn_{50}$ and $Cu_{75}Au_{25}$ alloys as a function of the number of atoms in the supercells. These supercells are constructed to have zero correlation functions for the first and second coordination shells, while the correlation functions for the following coordination shells are allowed to be arbitrary. In fact, they turn out to be close to those of the random alloy due to the initial random mixing of atoms. We find that converged results are obtained with a LIZ of one shell of nearest neighbors for the Cu-Zn alloy, corresponding to 13 atoms in the LIZ, and with a LIZ of two shells of nearest neighbors for the Cu-Au alloy, corresponding to 19 atoms in the LIZ. When the number of atoms in the supercell subsequently is changed for a fixed number of atoms in the LIZ we find for both alloys that the total energy of the supercell with only 32 atoms is within 0.1 mRy of the result for supercell with 256 atoms. Since the distributions of atoms in the different supercells are by construction different, these results confirm the SQS approach to the averaging problem described in Sec. IV.

B. Timing of the LSGF method

As already discussed in Sec. II C, the computational effort of the LSGF method is expected to scale as $O(N)$. That this

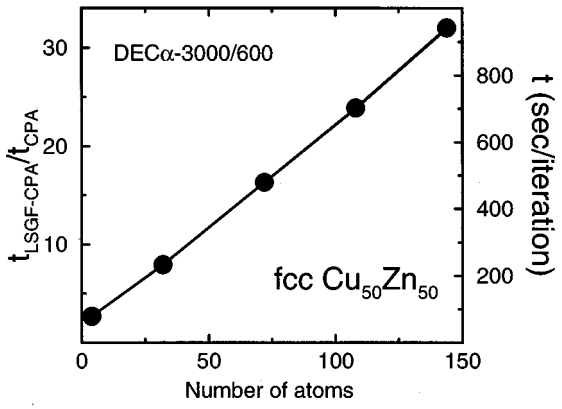

FIG. 4. Elapsed time for the LSGF-CPA calculations for a random fcc $Cu_{50}Zn_{50}$ alloy with the Wigner-Seitz radius $R_{WS}=2.70$ a.u. as a function of the number of atoms in the system. Two time scales are used. The left axis shows the time per LSGF-CPA iteration normalized to that of the conventional LMTO-CPA method and the right axis denotes real time in seconds per iteration. The local interaction zone consists of one shell of nearest neighbors (13 atoms).

is indeed true is illustrated in Fig. 4, where we plot the computer time per LSGF iteration as a function of the size of the supercell for the fcc $Cu_{50}Zn_{50}$ alloy. In these calculations we used a LIZ consisting of only one shell of nearest neighbors, which is sufficient for convergence in the LIZ size. However, an increase in the size M of the LIZ leads only to an increase in slope, reflecting the $O(M^3)$ prefactor in the scaling, but does not influence the linear behavior seen in Fig. 4. To make the computer time-scale machine independent we have normalized the time per LSGF iteration to that of a conventional CPA iteration. It is worth mentioning that not only do we find a linear increase in the computational effort with increasing system size, but we also find that in the limit of a small supercell the LSGF to CPA time ratio approaches unity. In fact, the absolute time per LSGF iteration is quite reasonable even though we have used only a moderately efficient work station. Note that, due to the efficient ''two-step'' iteration procedure described in the Appendix, we do not need more than 10–20 iterations to reach 10^{-6} Ry convergence.

To implement an $O(N)$ method one typically introduces extra computational steps, which for small supercell sizes make the method less efficient than the conventional $O(N^3)$ method. The question is therefore at which cell size the crossover occurs. As we shall see, the LSGF method may in favorable cases, depending on the kinds of atoms in the system, be as efficient as conventional techniques already for one atom per unit cell. To analyze the question we have performed a series of test calculations, but before we discuss these in detail we point out that the comparison we make obviously is computer-code dependent simply because the codes even for the same LMTO method have slightly different efficiencies. To represent a conventional band structure program we have used the LMTO Green's-function (GF) method described in Ref. 31, which allows us to treat ordered compounds and random alloys, in the framework of the CPA, on an equal footing. Due to a two-step iteration procedure, this code is approximately as efficient as the conventional LMTO code in the Hamiltonian formulation.[27]

TABLE I. Estimated number of atoms in the supercell N_{min} at which the LSGF method becomes more efficient than the LMTO-GF method as a function of the number of atoms M in the local interaction zone for a fcc underlying lattice.

Number of shells	M	N_{min}
0	1	1
1	13	2
2	19	4
3	43	28
4	55	45
5	79	86
6	87	101

If we neglect that part of the LSGF problem that is connected with the determination of the effective medium (see Sec. II D), the computer time for the LSGF and the LMTO-GF method may be written as

$$t_{LSGF}=\alpha NM^3 \tag{26}$$

and

$$t_{LMTO\text{-}GF}=\beta KN^3, \tag{27}$$

respectively, where α,β are proportionality constants, N is the number of atoms in the system, M is the size of the LIZ, and K is the number of k points in the Brillouin zone for the supercell. The latter may decrease with increasing N, so for a while the scaling of the LMTO-GF technique is in fact $O(N^2)$ rather than $O(N^3)$. However, we do not believe that K should be much smaller than 10 and therefore assume the estimate

$$K=\frac{300}{N}+10. \tag{28}$$

From our test calculations we have determined $\alpha/\beta\sim 1/5$, which together with Eqs. (26)–(28) leads to the following estimate for the number of atoms $N_{\min}$ in the supercell for which the LSGF method becomes more efficient than the LMTO-GF method:

$$N_{\min}=\sqrt{225+M^3/50}-15. \tag{29}$$

Values for $N_{\min}$ as a function of the LIZ size M are listed in Table I for the fcc structure. The calculations to be presented in Sec. VI show that we need to include at most three to four coordination shells in the LIZ to obtain a total energy with an accuracy of 0.1 mRy. It therefore follows from Table I that if we need a 100-atom supercell we are always in the regime where the LSGF method is substantially more efficient than conventional band structure calculations.

In the analysis presented above we did not consider the use of a parallel computer. It is in fact not easy to create efficient parallel algorithms for conventional band structure methods because the only obvious choice is a parallelization in k points and when a minimal number of such points is used the application of parallel computers becomes ineffi-

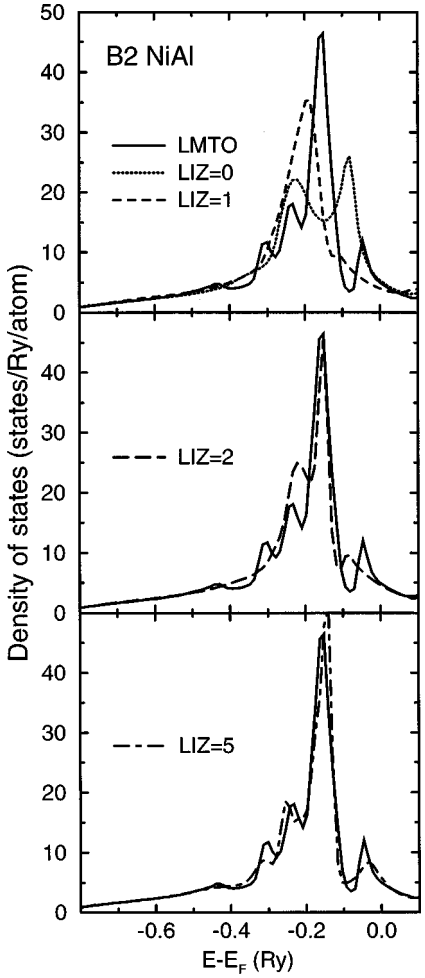

FIG. 5. Density of states for the ordered $B2$ NiAl alloy calculated by the LSGF-CPA method with different numbers of neighboring shells included in the LIZ. LIZ=0 corresponds to the single-site LIZ. The fully converged density of states calculated by the conventional LMTO-GF technique is also shown in each panel as a full line.

cient. In contrast, the LSGF method allows for an efficient parallelization in the sites of the supercell, exactly as in the LSMS method. This point has been thoroughly discussed by Wang *et al.*[20]

VI. RESULTS AND DISCUSSION

In this section we discuss several aspects of the LSGF method on the basis of calculations for a number of suitably chosen alloy systems. In particular, we discuss the two central concepts: the local interaction zone and the effective medium.

A. The local interaction zone concept: Ordered $B2$ NiAl alloy

As stated in Sec. II C, the concept of a local interaction zone is based on the suggestion that the site-diagonal blocks of the Green's function or, equivalently, the local density of states (DOS) for a particular atom within a large condensed system may be obtained by considering only the electronic multiple scattering processes in a finite spatial region, the LIZ, centered at that atom. In Fig. 5 we illustrate how well

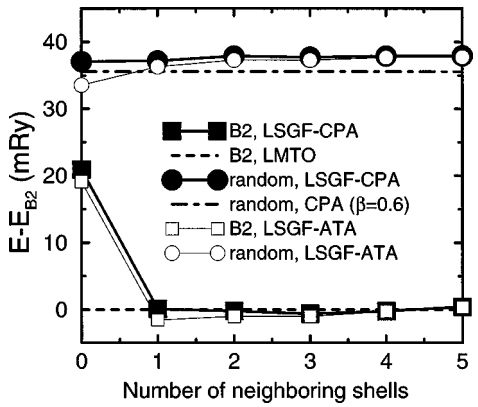

FIG. 6. Total energies of ordered ($B2$ structure, squares) and random (circles) bcc $Ni_{50}Al_{50}$ alloys ($R_{WS}=2.65$ a.u.) as a function of the number of neighboring shells included in the local interaction zone. Values obtained by the LSGF-CPA (filled symbols) and by the LSGF-ATA (open symbols) calculations are shown together with the reference calculations presented as a dashed line (LMTO, ordered sample) and a dot-dashed line (LMTO-CPA, random sample). The LSGF calculations for the random alloy have been performed for a supercell with 128 atoms. The LMTO-CPA calculations employed the screened impurity model (SIM) (Ref. 53) to account for the large charge transfer effects in NiAl alloy, and a prefactor $\beta=0.6$ was used.

the concept works by comparing the DOS calculated for an ordered $B2$ NiAl alloy by means of the LSGF-CPA method for different LIZ sizes with the result of a conventional LMTO-GF calculation. The underlying lattice in the LSGF calculations is bcc and the NiAl system is chosen because it exhibits the slowest convergence with LIZ size among all the alloys we have considered so far.

We observe in Fig. 5 that a single-site LIZ, i.e., a LIZ consisting of only the central atom and zero shells of nearest neighbors, leads to a qualitatively incorrect electronic structure. In fact, we obtain a DOS with a two-peak structure typical of a random bcc alloy. This is not surprising because in the single-site approximation the electronic spectrum reflects mainly the properties of the effective medium, which is an effective medium for a random alloy. In contrast, the DOS calculated by the LMTO-GF method, which is the converged result, has a pronounced peak positioned in a valley between the two random alloy peaks. If we now include the first shell of nearest neighbors in the LIZ, the LSGF-CPA DOS shows a single-peak structure in much better agreement with the LMTO-GF calculations. As the size of the LIZ increases the agreement between two methods gradually improves to the extent that for five shells of nearest neighbors the density of states calculated by the LSGF-CPA is well converged.

The relatively slow convergence of the density of states with respect to the size of the LIZ may be contrasted with the convergence of the total energy for the $B2$ NiAl alloy shown in Fig. 6. In the case of the ordered atomic distribution only the single-site LSGF-CPA result is more than 20 mRy in error and already from a one-shell LIZ the difference is less than 1 mRy/atom. This result reflects the variational principle, which ensures that the total energy converges over a length scale determined by the perturbation of the potential.[26] As discussed in Sec. II E, this length scale may

be estimated from the decay of the effective pair interactions and is quite dependent on the atomic species forming the alloy. In contrast, the density of states does not obey a variational principle and the convergence may be much slower than that of the total energy.

The total energy of a random distribution of 50% Ni and 50% Al atoms on the bcc lattice of a 128-atom supercell converges even faster than that of the ordered alloy; see Fig. 6. We notice that the large and negative ordering energy in the NiAl alloy is correctly reproduced. Further, our result for the random alloy is in good agreement with that obtained by the LMTO-CPA method in conjunction with the screened impurity model (SIM) CPA using a prefactor $\beta=0.6$.[53,42] The SIM allows us to account approximately for the charge transfer effects that are neglected in the conventional CPA, but of course correctly included in the LSGF-CPA calculations. Finally, we observe in Fig. 6 that the total energy of the random alloy is very well reproduced already for a single-site LIZ. This confirms our expectation that the CPA-like effective medium is a particularly good choice, at least for a random alloy.

B. Use of different effective media

The second important component of the LSGF method is the effective medium, the role of which is to reduce the size of the LIZ by improving the boundary condition for the finite region where the multiple scattering problem is solved exactly. This means, in particular, that LSGF calculations with different effective media must converge to the same result but with different LIZ sizes. This is illustrated in Fig. 6, which includes results obtained by an ATA effective medium constructed by assuming that the potential function $\tilde{P}_\alpha$ for the effective scatterers on the α sites is given by the average

$$\tilde{P}_\alpha^{-1}=(N_\alpha)^{-1}\sum_{R\in\alpha}P_R^{-1}, \tag{30}$$

with a similar expression for the potential function on the β sites. Hence we do not solve Eqs. (15) but obtain the Green's function for the effective scatterers from $\tilde{P}-\mathbf{S}$.

One may see in the figure that for the five-shell LIZ the two different effective media give essentially the same results for both the ordered and the random phases. However, the results obtained by the LSGF-CPA are somewhat more stable and converge faster than those of the LSGF-ATA. In particular, the total energy of the random alloy for the single-site LIZ and the ATA effective medium is substantially smaller than that obtained by the CPA effective medium. Note that the time one needs to solve the CPA equations (15) is not a dominant part of the calculations and one does not save a substantial amount of time by substituting the CPA effective medium by the ATA effective medium, especially when the LIZ is large. In fact, the decrease of the LIZ size one may obtain within the LSGF-CPA compared to the LSGF-ATA will more than compensate for the time spent in solving the CPA equations.

In the case of bcc NiAl, for instance, it is sufficient to use a LIZ of one shell of nearest neighbors and the CPA effective medium if the accuracy one is interested in is of the order of 1 mRy (or about 2% of the ordering energy). At the same time within the LSGF-ATA one has to go to two or three shells of nearest neighbors to obtain the same accuracy. Of course, one may save a little time by applying the ATA effective medium for the five-shell LIZ if higher accuracy is needed. However, in that case there is a better way to solve the problem, and we will illustrate this by the example of the off-stoichiometric partially ordered bcc $Ni(Ni_{9.375}Al_{90.625})$ alloy.

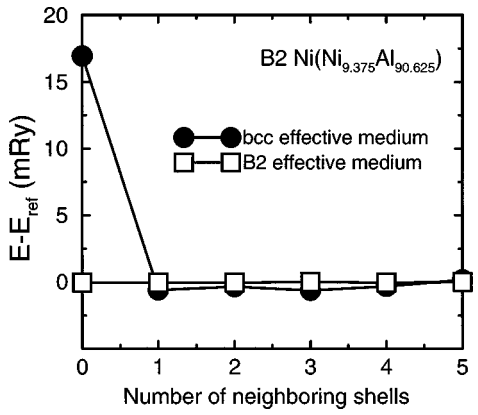

FIG. 7. Total energy of a partially ordered $B2$ $Ni(Ni_{9.375}Al_{90.625})$ alloy ($R_{WS}=2.65$ a.u., 128 atomic supercell) as a function of the number of neighboring shells included in the local interaction zone. Values obtained by the LSGF-CPA calculations with effective atoms of one kind placed in a bcc underlying lattice (filled circles) and with effective atoms of two kinds placed in a $B2$ underlying lattice (open squares) are shown. The reference energy E_{ref} is the converged result (five shells) for the $B2$ effective medium.

When there is an excess of Ni atoms in a partially ordered $B2$ NiAl alloy these atoms are known experimentally to occupy Al sites, while the Ni sublattice is completely ordered and occupied only by Ni atoms. As we have already mentioned in Sec. II D, to deal with such a system we have two possible choices for the underlying lattice. Either we consider it as a bcc lattice with just one atom per unit cell or we treat it closer to the real situation, namely, as a $B2$ lattice with two different sublattices and, of course, two types of effective atoms. By definition a single-site LIZ will suffice for ordered NiAl. In Fig. 7 we show how the total energy of partially ordered $Ni(Ni_{9.375}Al_{90.625})$ converges with respect to the size of the LIZ for the bcc and $B2$ effective medium. It is clearly seen that by making the effective medium slightly more complicated the size of the LIZ is substantially reduced and we obtain an accurate result already for a single-site LIZ. It is also seen that for a larger LIZ the two effective media lead to the same result.

The examples in this section demonstrate the possibility to vary the effective medium to suit the problem at hand and in particular to minimize the size of the LIZ and thereby the computational effort. The examples also demonstrate that the final results are independent of the choice of effective medium, as should be the case.

C. Total energy calculations for a general atomic distribution: Rh-Pd alloy

To illustrate the possibility to calculate accurate total energies for systems with any distribution of atoms on the un-

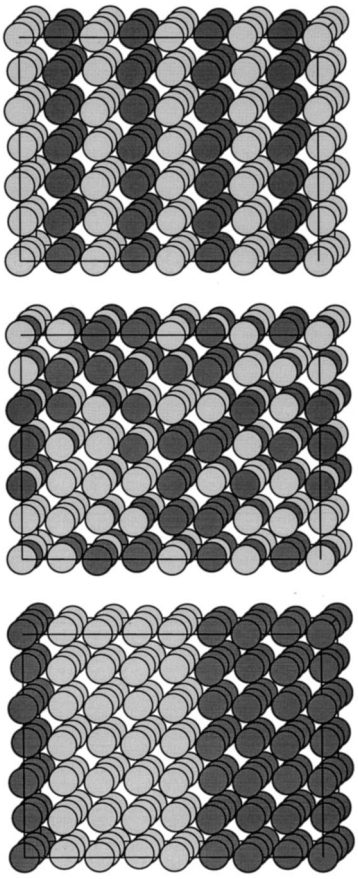

FIG. 8. Three different distributions of Rh (dark gray) and Pd (light gray) atoms in an equiatomic fcc Rh-Pd alloy. The ordered sample ($L1_0$ structure, top), the random sample (middle), and the segregated sample (bottom) were constructed on the fcc underlying lattice for the 144-atom supercell. The values of the short-range order parameter for each of these structures are given in Table II.

derlying lattice by means of the LSGF-CPA method we have performed self-consistent calculations for the fcc $Rh_{50}Pd_{50}$ alloy with three different atomic configurations: completely ordered in the $L1_0$ structure, completely random, and segregated. We have considered a supercell with 144 atomic sites, periodic boundary conditions, and the atomic distributions shown in Fig. 8. In setting up a particular atomic distribution we have specified the first five Warren-Cowley short-range-order parameters α_i, (Ref. 40) according to the values in Table II. In particular, for the segregated sample shown in the lower panel of Fig. 8, α_i is positive up to the fifth shell, indicating good phase separation. The results of the LSGF-CPA calculations are then compared with those of the LMTO Green's function method for an ordered sample, as

TABLE II. Warren-Cowley short-range-order parameters α_i for the first five shells in three fcc Rh-Pd samples shown in Fig. 8.

	α_i, $i=1-5$				
Sample	1	2	3	4	5
ordered, $L1_0$	$-1/3$	1	$-1/3$	1	$-1/3$
random	0	0	0	0	0
segregated	2/3	2/3	1/3	1/3	1/3

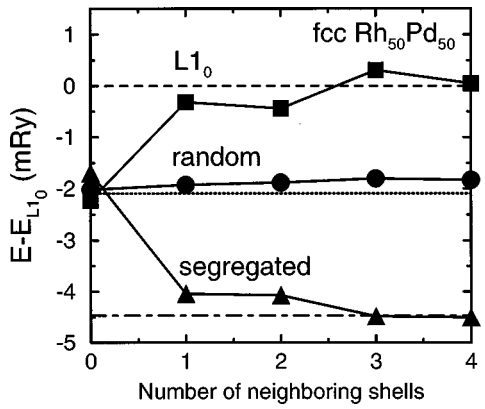

FIG. 9. Total energies of ordered ($L1_0$ structure, squares), random (circles), and segregated (triangles) fcc $Rh_{50}Pd_{50}$ alloys ($R_{WS}=2.92$ a.u.) as a function of the number of neighboring shells included in the local interaction zone. Supercells are shown in Fig. 8. Values obtained by the LSGF-CPA method are shown by filled symbols and full lines. The energies obtained by the reference calculations are shown by a dashed line (LMTO, ordered sample), a dotted line (LMTO-CPA, random sample), and a dot-dashed line (interface Green's function technique, segregated sample).

well as with LMTO-CPA results for the random samples. We expect the CPA to give reliable total energies for Rh-Pd alloys independent of the value of the prefactor β used in the screened impurity model because the charge transfer in this system is very small. Finally, the segregated sample is made up from four (010) layers of pure Rh and four (010) layers of pure Pd and its total energy may be calculated not only by the LSGF method but also by the interface Green's function technique.[37]

In Fig. 9 we show the total energies of the three samples as a function of the number of neighboring shells included in the LIZ. In agreement with the experimental phase diagram for the Rh-Pd system, which has a miscibility gap, we find the segregated sample to have the lowest total energy. Then follows the random alloy, and the ordered phase has the highest total energy. The excellent real-space convergence of the LSGF-CPA method may again be judged from Fig. 9. We observe that already for the LIZ that includes just one shell of nearest neighbors, i.e., 13 atoms, the total energies are converged to within 0.5 mRy, and for four shells the difference between the LSGF method and the reference calculations, i.e., bulk LMTO and interface Green's function technique, is below 0.1 mRy. The difference between the LSGF and CPA calculations is expected to be larger, and as a matter of fact one may judge the accuracy of the latter rather than the former from this comparison.

We note that the LSGF method allows us to obtain reliable total energies for systems that normally would have been treated by three different techniques, e.g., the bulk LMTO, the LMTO-CPA, and the interface LMTO Green's function techniques. Moreover, the LSGF method allows us to consider *any* atomic distribution on the underlying lattice. Therefore, the total energy of a large class of important alloy systems may be treated on the same footing by means of a single computational technique thereby adding to the faith in the results.

In Fig. 9 one observes a stepwise behavior of the total energy as a function of the LIZ size for the ordered and the

segregated samples. Thus the change in the total energy is largest when we include the first shell of neighbors, almost zero when we include the second and the fourth shells, and slightly nonzero when we include the third shell. This convergence behavior of the LSGF-CPA method may be described in terms of the effective pair interactions discussed in Sec. II E. In the present Rh-Pd alloy system Wolverton *et al.*[54] found effective pair interactions that were appreciable for the first and third coordination shells but small for the second and fourth shells, in complete agreement with the convergence pattern shown in Fig. 9. This is not a coincidence and in all the cases considered in the present paper we find that the convergence in terms of the LIZ size follows the range of the effective pair interactions.

One also observes in Fig. 9 that the total energy of the random sample, as in the case of the Ni-Al alloy, converges faster than for the ordered and segregated samples, indicating that the CPA effective medium in fact forms a perfect representation of the average of a random atomic distribution. Finally, when we compare only the ordered and the segregated samples we observe that these two samples exhibit similar convergence properties with respect to the size of the LIZ. This means that we do not have to test the convergence for each new atomic distribution but only for, e.g., the ordered sample.

D. Convergence in real space: Ordering energies of alloys

In Fig. 10 we present convergence tests for different alloy systems, fcc $Cu_{75}Zn_{25}$, $Cu_{75}Au_{25}$, $Cu_{50}Au_{50}$, $Ni_{75}Al_{25}$, and bcc $Li_{50}Mg_{50}$ and $W_{50}Al_{50}$. Here we have calculated the total energy of two phases, the random and the simplest ordered phase for a given concentration, i.e., $L1_2$ or $L1_0$ for the fcc alloys and $B2$ for the bcc alloys. In addition to the LSGF calculations, the ordered samples have also been treated by the LMTO-GF technique and the energies obtained in the latter calculations serve as reference.

In Fig. 10 it is seen that already for a single-shell LIZ all alloys, except W-Al, are converged to within 1 mRy. Moreover, in Sec. V B it is shown that the LSGF technique is most efficient when the size of the LIZ does not exceed three or four shells of nearest neighbors for the fcc underlying lattice and five shells for the bcc underlying lattice. For LIZ's of these sizes we see in the figure that the total energy for all alloy systems including the ordered samples are converged to within 0.1 mRy. This conclusion does not depend on whether we deal with alloys of transition or of simple metals, with large or small charge transfers, or with systems that have a tendency towards order or phase separation. Also, it does not depend on the alloy concentration, as illustrated by the examples of Cu-Zn (Ref. 55) and Cu-Au alloys. Finally, the numerical tests, including the results for the bcc and partially ordered $B2$ NiAl alloys and for the Rh-Pd alloys presented in previous sections, cover a broad spectrum of systems and we believe our results demonstrate the general applicability of the LSGF method.

Finally, we note that in all the cases considered in the present study we correctly reproduce the ordering tendencies. Thus, for Cu-Zn, Cu-Au, Ni-Al, and Li-Mg alloys we find that the ordered phase has a lower energy than the random phase, while for the Rh-Pd and W-Al alloys we find that the

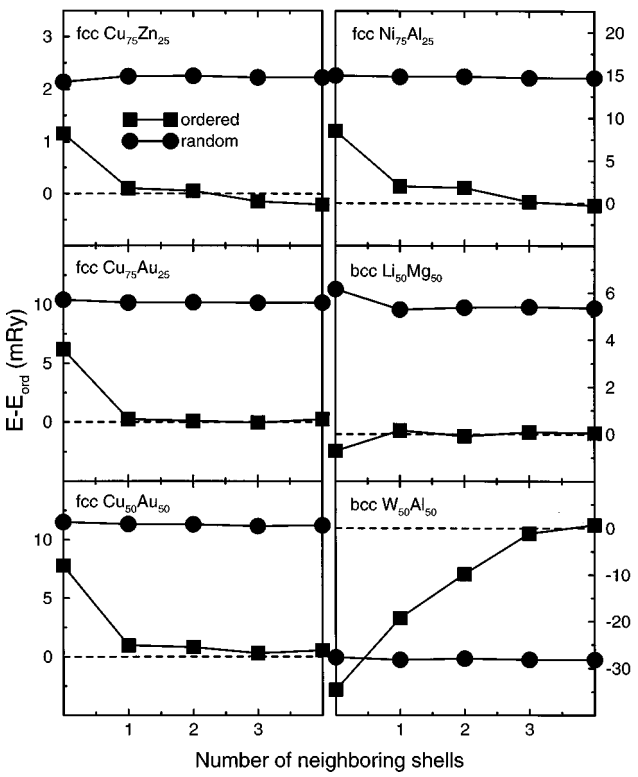

FIG. 10. Total energies of simplest ordered phases ($L1_2$ for fcc $A_{75}B_{25}$, $L1_0$ for fcc $A_{50}B_{50}$, and $B2$ for bcc $A_{50}B_{50}$ alloys) shown as squares and random phases (circles) as a function of the number of neighboring shells included in the local interaction zone for different alloy systems. Values are given relative to the results of conventional LMTO-GF calculation for the corresponding ordered phase.

ordered phase has a higher energy than the random phase. Experimentally, it is known that the stability of the ordered phases is very high in Ni-Al and intermediate in Cu-Au, while no ordered phases are formed for fcc $Cu_{75}Zn_{25}$ and bcc $Li_{50}Mg_{50}$. The values for the ordering energies found in our calculations are in qualitative agreement with this trend. However, it should be noted that in Fig. 10 we present the total energies of the random and ordered phases at the same lattice parameter, while in fact the degree of order may influence the interatomic distances.[42] On the other hand this effect is usually small and it is unlikely that it will substantially change the results shown in Fig. 10.

VII. SUMMARY

We have presented and discussed the order-N LSGF method for electronic structure calculations in systems with many atoms distributed arbitrarily on an underlying crystal lattice. The method is formulated in the framework of the LMTO-GF technique and is based on the local interaction zone concept. Each local interaction zone is embedded in an effective medium, and we find that the CPA effective medium for a multicomponent alloy where each atom of the original supercell is considered to be an independent component of a completely random alloy on the same underlying lattice forms an optimal effective medium. The method has been applied in total energy calculations for a number of

different substitutional alloys with different degrees of order and is found to exhibit rapid convergence in terms of the size of the local interaction zone. In general the method yields results in excellent agreement with those obtained by alternative first-principles techniques. The number of atoms for which the LSGF method becomes more efficient than conventional band structure methods lies in the range 1–50 for all the systems considered in the present work. The exact figure depends on the degree of order, the required accuracy, and the atomic species forming the alloy. This latter convergence dependence in terms of the atomic species is found to be accurately characterized by the range of the so-called effective cluster interactions (ECI's), and we find that the real-space convergence of the LSGF method is directly determined by the convergence of the ECI's in the system.

ACKNOWLEDGMENTS

The Swedish Material Consortium No. 9 and NFR Grant No. 9871-321 are gratefully acknowledged. The Center for Atomic-Scale Materials Physics is sponsored by the Danish National Research Foundation.

APPENDIX: EFFECTIVE TWO-STEP PROCEDURE FOR THE CHARGE SELF-CONSISTENCY AND THE SOLUTION OF THE CPA EQUATION

In this appendix we discuss one way to accelerate electronic structure calculations based on the Green's function technique. The actual equations are written in an LMTO basis, but a generalization to any other basis, e.g., KKR, is straightforward.

The most time-consuming step of all first-principles reciprocal-space-based one-electron methods is the integration over the Brillouin zone, which is needed, for instance, when calculating the KKR-ASA Green's function in Sec. II B. This problem becomes even more serious in the calculations of random alloys within the framework of the CPA. In that case the k-space integration has to be repeated several times at each complex energy (and at the same LDA iteration) during the iterative solution of the CPA equation.

In conventional LMTO calculations[27] the number of time-consuming band iterations is greatly reduced by the LMTO scaling principle. For surface calculations one may introduce a similar technique based on the solution of the linearized Dyson equation, which reduces the number of times the complete Dyson equation must be solved by one order of magnitude.[38] The principle is that the complete electronic structure is only recalculated when charge self-consistency has been obtained by means of an approximate state density or Green's function.

In Green's function calculations we find the following ''two-step'' scheme to be very efficient. The Green's function at the $(n+1)$th iteration is related to that at the nth iteration by the Dyson equation

$$\mathbf{g}^{(n+1)}(z)=\mathbf{g}^{n}(z)+\mathbf{g}^{n}(z)[P^{n}(z)-P^{(n+1)}(z)]\mathbf{g}^{(n+1)}(z), \tag{A1}$$

which must be solved for each complex energy and either for each $\mathbf{k}$ point in the Brillouin zone or for an infinitely large cluster in real space. We now assume that a good approximation to the complete solution of Eq. (A1) is given by the single-site cluster in real space, i.e., we replace Eq. (A1) by

$$\mathbf{g}_{RR}^{(n+1)}(z)=\mathbf{g}_{RR}^{n}(z)+\mathbf{g}_{RR}^{n}(z)[P_{R}^{n}(z)-P_{R}^{(n+1)}(z)]\mathbf{g}_{RR}^{(n+1)}(z), \tag{A2}$$

where the initial value of $\mathbf{g}_{RR}^{n=1}$ is the on-site Green's function given by the complete Brillouin zone integral or by the LSGF, Eq. (14). The smaller the difference in potential functions between different iterations, the better the approximation works. In fact, at self-consistency

$$\Delta P_{R}=P_{R}^{n}-P_{R}^{(n+1)}\rightarrow 0 \tag{A3}$$

and the single-site approximation (A2) to Eq. (A1) becomes exact.

Within this approximation one may find an analytical solution to the CPA equation. Suppose we have obtained the Green's functions $\tilde{g}_{\alpha\alpha}$ and $g_{R\alpha}^{0}$ in Eq. (15) using some guess for $\tilde{P}$. We now choose the potential function for the next CPA iteration in the form

$$\tilde{P}_{\alpha}^{new}(z)=\tilde{P}_{\alpha}(z)+\{\langle g_{\alpha\alpha}^{0}\rangle^{-1}-[\tilde{g}_{\alpha\alpha}(z)]^{-1}\} \tag{A4}$$

and calculate the new effective medium Green's function $\tilde{g}_{\alpha\alpha}^{new}$ from Eq. (A2) and insert into Eq. (15), which shows that

$$g_{R\alpha}^{0,new}(z)=g_{R\alpha}^{0}(z). \tag{A5}$$

Therefore, from the Eqs. (A2), (A4), and (A5) we may write, omitting subsript α (or β),

$$\begin{aligned}\tilde{g}^{new}(z)&=[1-\tilde{g}(z)\Delta\tilde{P}(z)]^{-1}\tilde{g}(z)\\&=(1+\tilde{g}(z)\{\langle g(z)\rangle^{-1}-[\tilde{g}(z)]^{-1}\})^{-1}\tilde{g}(z)\\&=\langle g(z)\rangle=\langle g^{new}(z)\rangle,\end{aligned} \tag{A6}$$

which means that the CPA condition given by the third of Eqs. (15) is fulfilled. Although Eq. (A2) is only an approximation, and therefore Eqs. (A5) and (A6) do not hold exactly, the updating of the coherent potential function by Eq. (A4) gives us a very rapid convergence when solving the CPA equation (15). We never need more than five CPA iterations to solve the CPA equation with a reasonable accuracy. In fact, there is no need for a very high accuracy at the beginning of the LDA self-consistency iterations, and towards the end the approximation (A2) to Eq. (A1) and therefore also Eq. (A4) becomes increasingly accurate.

During the iterations toward the LDA self-consistency we also use Eq. (A2). First we solve the complete set of LSGF equations, the so-called big iteration. We then perform ''small'' LDA iterations, typically between 40 and 300 depending on the problem, with a small admixture, typically 1–5%, of a new charge density. During these iterations we determine the on-site element of the Green's function at each site g_{RR} by solving only Eq. (A2). When the small iterations are converged, we perform the next big iteration. At this step it may be desirable to mix the potentials between different big iterations, typically 70% of the new potential, and to

keep a minimal number of small iterations, between 10 and 20, to compensate for the small mixing close to the end of the self-consistent procedure. Note that a completely analogous two-step procedure may be used in any calculations based on a Green's function approach. In particular, it is used in our bulk and interface CPA Green's function codes.[31]

We illustrate the efficiency and the accuracy of the two-step approach by LMTO-CPA Green's function calculations for a partially ordered $(Ni_{92}Hf_{08})_3Al$ alloy in the $L1_2$ structure. The self-consistency criterion for the total energy was 10^{-6} Ry/atom. The one-step calculations required 118 (big) iterations and gave a total energy of $-56.379\,166$ Ry/atom, while the two-step procedure converged after 18 (big) iterations and gave a total energy of $-56.379\,177$ Ry/atom.

[1] P. Hohenberg and W. Kohn, Phys. Rev. **136B**, 864 (1964).

[2] W. Kohn and L. J. Sham, Phys. Rev. **140**, A1133 (1965).

[3] W. Yang, Phys. Rev. Lett. **66**, 1438 (1991); T. Zhu, W. Pan, and W. Yang, Phys. Rev. B **53**, 12 713 (1996).

[4] G. Galli and M. Parrinello, Phys. Rev. Lett. **69**, 3547 (1992); F. Mauri, G. Galli, and R. Car, Phys. Rev. B **47**, 9973 (1993); F. Mauri and G. Galli, *ibid.* **50**, 4316 (1994).

[5] P. Ordejón, D. A. Drabold, M. P. Grumbach, and R. M. Martin, Phys. Rev. B **48**, 14 646 (1993); P. Ordejón, D. A. Drabold, R. M. Martin, and M. P. Grumbach, *ibid.* **51**, 1456 (1995); S. Itoh, P. Ordejón, D. A. Drabold, and R. M. Martin, *ibid.* **53**, 2132 (1996); P. Ordejón, E. Artacho, and J. M. Soler, *ibid.* **53**, R10 441 (1996).

[6] W. Kohn, Chem. Phys. Lett. **208**, 167 (1993).

[7] E. B. Stechel, A. R. Williams, and P. J. Feibelman, Phys. Rev. B **49**, 10 088 (1994); W. Hierse and E. B. Stechel, *ibid.* **50**, 17 811 (1994).

[8] X.-P. Li, R. W. Nunes, and D. Vanderbilt, Phys. Rev. B **47**, 10 891 (1993).

[9] M. S. Daw, Phys. Rev. B **47**, 10 895 (1993).

[10] S.-Y. Qiu, C. Z. Wang, K. M. Ho, and C. T. Chan, J. Phys.: Condens. Matter **6**, 9153 (1994).

[11] E. Hernandez and M. J. Gillan, Phys. Rev. B **51**, 10 157 (1995); E. Hernandez, M. J. Gillan, and C. M. Goringe, *ibid.* **53**, 7147 (1996).

[12] A. E. Carlsson, Phys. Rev. B **51**, 13 935 (1995).

[13] S. Goedecker and L. Colombo, Phys. Rev. Lett. **73**, 122 (1994); S. Goedecker and M. Teter, Phys. Rev. B **51**, 9455 (1995).

[14] A. P. Horsfield, A. M. Bratkovsky, M. Fearn, D. G. Pettifor, and M. Aoki, Phys. Rev. B **53**, 12 694 (1996).

[15] A. F. Voter, J. D. Kress, and R. N. Silver, Phys. Rev. B **53**, 12 733 (1996).

[16] D. A. Drabold and O. F. Sankey, Phys. Rev. Lett. **70**, 3631 (1993).

[17] J. R. Chelikovsky, N. Troullier, and Y. Saad, Phys. Rev. Lett. **72**, 1240 (1994).

[18] S. Baroni and P. Giannozzi, Europhys. Lett. **17**, 547 (1992).

[19] D. M. C. Nicholson, G. M. Stocks, Y. Wang, W. A. Shelton, Z. Szotek, and W. M. Temmerman, Phys. Rev. B **50**, 14 686 (1994).

[20] Y. Wang, G. M. Stocks, W. A. Shelton, D. M. C. Nicholson, Z. Szotek, and W. M. Temmerman, Phys. Rev. Lett. **75**, 2867 (1995).

[21] I. A. Abrikosov, A. M. N. Niklasson, S. I. Simak, B. Johansson, A. V. Ruban, and H. L. Skriver, Phys. Rev. Lett. **76**, 4203 (1996).

[22] W. Kohn, Phys. Rev. Lett. **76**, 3168 (1996).

[23] O. K. Andersen, Phys. Rev. B **12**, 3060 (1975).

[24] O. K. Andersen and O. Jepsen, Phys. Rev. Lett. **53**, 2571 (1984).

[25] O. K. Andersen, O. Jepsen, and D. Glötzel, in *Highlights of Condensed-Matter Theory*, edited by F. Bassani, F. Fumi, and M. P. Tosi (North-Holland, New York, 1985).

[26] O. Gunnarsson, O. Jepsen, and O. K. Andersen, Phys. Rev. B **27**, 7144 (1983).

[27] H. L. Skriver, *The LMTO Method* (Springer-Verlag, Berlin, 1984).

[28] R. Podloucky, R. Zeller, and P. H. Dederichs, Phys. Rev. B **22**, 5777 (1980); B. Drittler, M. Weinert, R. Zeller, and P. H. Dederichs, *ibid.* **39**, 930 (1989)

[29] C. Koenig, N. Stefanou, and J. M. Koch, Phys. Rev. B **33**, 5307 (1986).

[30] D. D. Johnson, D. M. Nicholson, F. J. Pinski, B. L. Gyorffy, and G. M. Stocks, Phys. Rev. Lett. **56**, 2088 (1986); D. D. Johnson, D. M. Nicholson, F. J. Pinski, B. L. Gyorffy, and G. M. Stocks, Phys. Rev. B **41**, 9701 (1990).

[31] I. A. Abrikosov and H. L. Skriver, Phys. Rev. B **47**, 16 532 (1993).

[32] If positions of atoms are shifted from the sites of the underlying lattice due to, for example, local lattice relaxations, this perturbation can be included in Eq. (14) through the difference between the real-space structure constant matrices for the original system $\mathbf{S}$ and for the underlying lattice $\widetilde{\mathbf{S}}$ as $\mathbf{g}(z)=\{[\widetilde{\mathbf{g}}(z)]^{-1}+[\mathbf{P}(z)-\widetilde{\mathbf{P}}(z)]-(\mathbf{S}-\widetilde{\mathbf{S}})\}^{-1}$. However, one must go beyond the ASA to consider such effects in practice.

[33] M. Aldén, I. A. Abrikosov, B. Johansson, N. M. Rosengaard, and H. L. Skriver, Phys. Rev. B **50**, 5131 (1994).

[34] W. Lambrecht and O. K. Andersen, Surf. Sci. **178**, 256 (1986); and private communication.

[35] J. E. Inglesfield and G. A. Benesh, Phys. Rev. B **37**, 6682 (1988).

[36] J. M. MacLaren, S. Crampin, D. D. Vvedensky, and J. Pendry, Phys. Rev. B **40**, 12 164 (1989).

[37] H. L. Skriver and N. M. Rosengaard, Phys. Rev. B **43**, 9538 (1991).

[38] H. L. Skriver and N. M. Rosengaard, Phys. Rev. B **46**, 7157 (1992).

[39] J. S. Faulkner, Prog. Mater. Sci. **27**, 1 (1982).

[40] F. Ducastelle, *Order and Phase Stability in Alloys* (North-Holland, Amsterdam, 1991).

[41] D. D. Johnson and F. J. Pinski, Phys. Rev. B **48**, 11 553 (1993).

[42] A. V. Ruban, I. A. Abrikosov, and H. L. Skriver, Phys. Rev. B **51**, 12 958 (1995).

[43] J. Hafner, *From Hamiltonians to Phase Diagrams* (Springer-Verlag, Berlin, 1987).

[44] D. G. Pettifor, *Bonding and Structure of Molecules and Solids* (Clarendon, Oxford, 1995).

[45] A. Zunger, in *Statics and Dynamics of Alloy Phase Transformations*, edited by P. E. A. Turchi and A. Gonis (Plenum, New York, 1994), p. 361.

[46] A. Gonis, X.-Z. Zhang, A. J. Freeman, P. Turchi, G. M. Stocks, and D. M. Nicholson, Phys. Rev. B **36**, 4630 (1983).

[47] J. W. D. Connolly and A. R. Williams, Phys. Rev. B **27**, 5169 (1983).
[48] J. Perdew and A. Zunger, Phys. Rev. B **23**, 5048 (1981).
[49] D. M. Ceperley and B. J. Alder, Phys. Rev. Lett. **45**, 566 (1980).
[50] A. Gonis, G. M. Stocks, W. H. Butler, and H. Winter, Phys. Rev. B **29**, 555 (1984).
[51] J. M. Sanchez, F. Ducastelle, and D. Gratias, Physica A **128**, 334 (1984).
[52] A. Zunger, S.-H. Wei, L. G. Ferreira, and J. E. Bernard, Phys. Rev. Lett. **65**, 353 (1990).
[53] P. A. Korzhavyi, A. V. Ruban, I. A. Abrikosov, and H. L. Skriver, Phys. Rev. B **51**, 5773 (1995); I. A. Abrikosov, Yu. H. Vekilov, P. A. Korzhavyi, A. V. Ruban, and L. E. Shilkrot, Solid State Commun. **83**, 867 (1992).
[54] C. Wolverton, D. de Fontaine, and H. Dreyssé, Phys. Rev. B **48**, 5766 (1993).
[55] The convergence for the $Cu_{50}Zn_{50}$ and $Rh_{75}Pd_{25}$ alloys was presented by us in Ref. 21.